



STRUCTURAL SCIENCE
CRYSTAL ENGINEERING
MATERIALS

Volume 70 (2014)

Supporting information for article:

Isomorphism and solid solution as shown by an accurate high-resolution diffraction experiment

Agnieszka Poulain, Maciej Kubicki and Claude Lecomte

Table S1. Rigid bond test for non-hydrogen atoms of 1a.

ATOM 1	ATOM 2	$Z_A^2 [\text{\AA}^2]$	$Z_B^2 [\text{\AA}^2]$	$\Delta Z_{AB}^2 [\text{\AA}^2]$
C1	N1	0.0101	0.0096	0.0005(2)
C1	C6	0.0111	0.0113	-0.0002(2)
C1	C2	0.0109	0.0111	-0.0002(2)
C2	C3	0.0126	0.0127	-0.0001(2)
C3	C4	0.0138	0.0139	-0.0001(2)
C4	Cl1	0.0105	0.0102	0.0003(1)
C4	C5	0.0127	0.0128	0.0000(2)
C5	C6	0.0116	0.0116	0.0000(2)
C7	N1	0.0111	0.0104	0.0007(2)
C7	N2	0.0110	0.0107	0.0003(1)
C7	C71	0.0120	0.0126	-0.0006(2)
C8	N8	0.0104	0.0105	-0.0002(1)
C8	N2	0.0149	0.0149	<0.0000(2)
C8	C9	0.0123	0.0124	-0.0002(2)
C9	Br1a	0.0124	0.0171	-0.0047(3)
C9	N1	0.0112	0.0111	0.0002(2)
C9	C91b	0.0122	0.0118	0.0005(2)
N8	O81	0.0183	0.0185	-0.0002(3)
N8	O82	0.0204	0.0208	-0.0004(3)
C91b	N91b	0.0119	0.0114	0.0005(2)

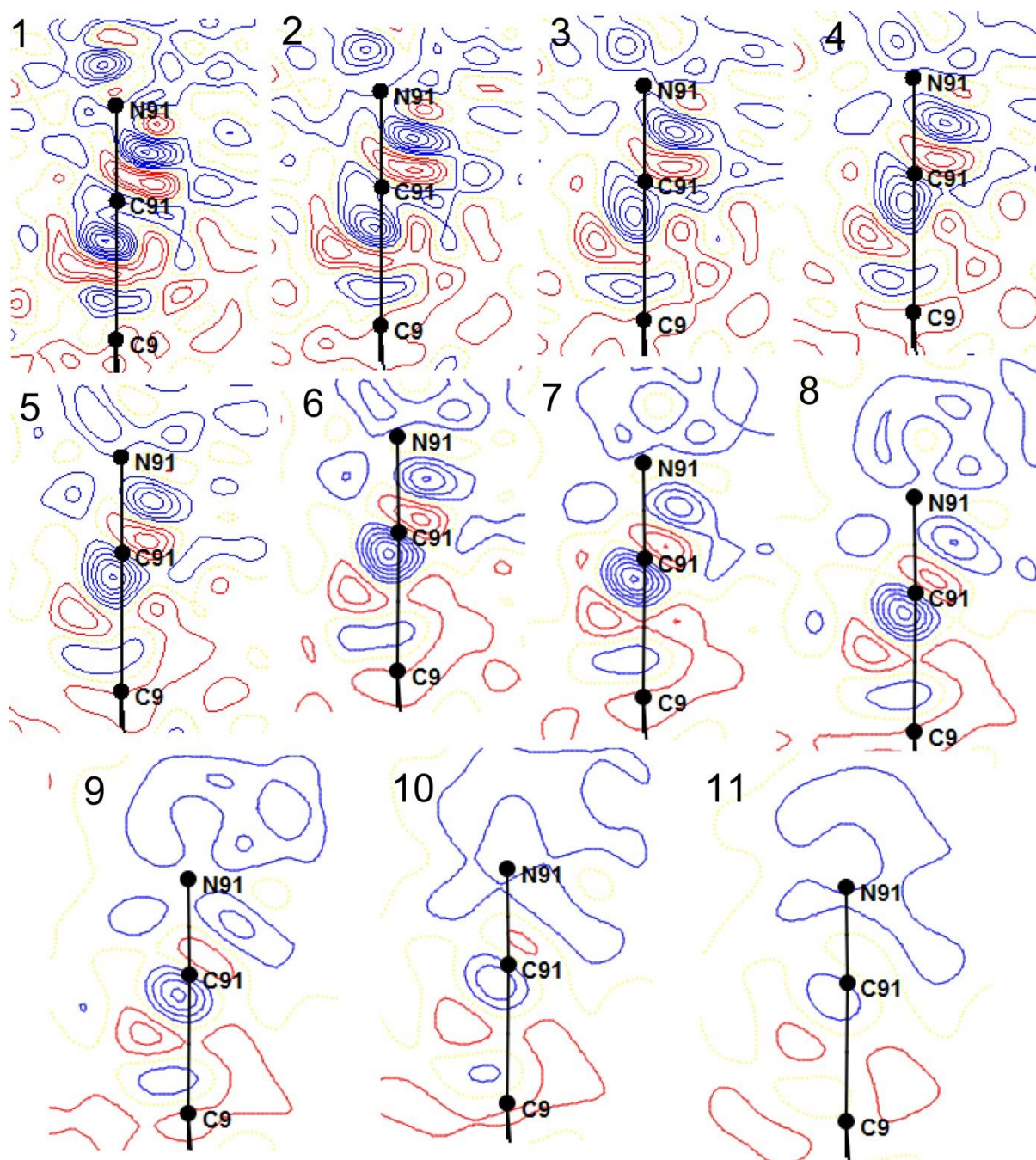


Figure S1. Residual Fourier density maps without bromine atom included in the model – after multipolar refinement (contour 0.05e/Å³, blue positive, red negative) – resolution changing from 1 (1.10Å⁻¹) to 11 (0.60Å⁻¹) every 0.05Å⁻¹.

Details of multipolar refinement:

The following multipolar refinement strategy was applied: scale factor was refined continuously with all parameters and the electroneutrality constraint was kept until the end of the refinement; high order refinement ($s > 0.7 \text{ \AA}^{-1}$) of coordinates and displacement parameters of non-H atoms (to ensure the deconvolution of the thermal motion from the deformation electron density [Hirshfeld, 1976]) was followed by low order refinement ($s < 0.7 \text{ \AA}^{-1}$) of H-atoms positions constrained to the values from neutron diffraction studies [Allen *et al.*, 2006] and initially with $U_{\text{iso}}(\text{H})$ constrained to $1.2U_{\text{eq}}(\text{C}_{\text{aromatic}})$ and $1.5U_{\text{eq}}(\text{C}_{\text{methyl}})$. Then the multipolar populations (P_{lm} 's) were refined for all ordered atoms against all reflections (hereafter $s = 1.13 \text{ \AA}^{-1}$, with $I > 2\sigma(I)$) with symmetry constraints generated automatically by MoPro according to the local orthogonal axis system ($3m$ for C71 atom, $m_y m_z$ for C1-C6, N1, N2 and N8 atoms, m_z for C7, C8, O81 and O82 atoms). Next, the valence populations and κ 's of all atoms were refined successively, with $\kappa_{\text{hyd}} = 1.16$ and $\kappa'_{\text{hyd}} = 1.20$ as the starting values and with restraint level $\sigma = 0.05$. Chemical equivalency constraints were kept on P_{val} , P_{lm} and κ 's, for: C2 = C6, C3 = C5, O81 = O82, H2 = H6, H3 = H5, H71 = H72 = H73 to reduce the number of variables and to guarantee the physical meaningfulness of the refined parameters. After reaching the convergence in constrained successive refinement of scale factor, P_{val} , P_{lm} , κ and κ' , the xyz and U_{ij} were included and refined against all reflections.

It appeared that a residual density up to $0.52(4)/-0.35(4) \text{ e/\AA}^3$ around the chlorine atom remains until the end of the refinement process. The arrangement of the negative and positive peaks (Fig. S2) observed only at high resolution ($> 0.75 \text{ \AA}^{-1}$) presented a shashlik-like pattern which has been recently indicated as a warning sign of atoms, for which harmonic motion model does not suffice [Meindl *et al.*, 2010; Henn *et al.*, 2010; Zhurov *et al.*, 2011, Paul *et al.*, 2011a, Poulain *et al.*, 2014]. Introduction of third order Gram-Charlier coefficients [Johnson & Levy, 1974; Sørensen *et al.*, 2003] significantly improved the residual density map, in particular lowered the residual peaks around chlorine atom (Fig. 3). Therefore anharmonicity was included in the high order refinement ($\sin\theta/\lambda > 0.7 \text{ \AA}^{-1}$) (see Poulain *et al.*, 2014).

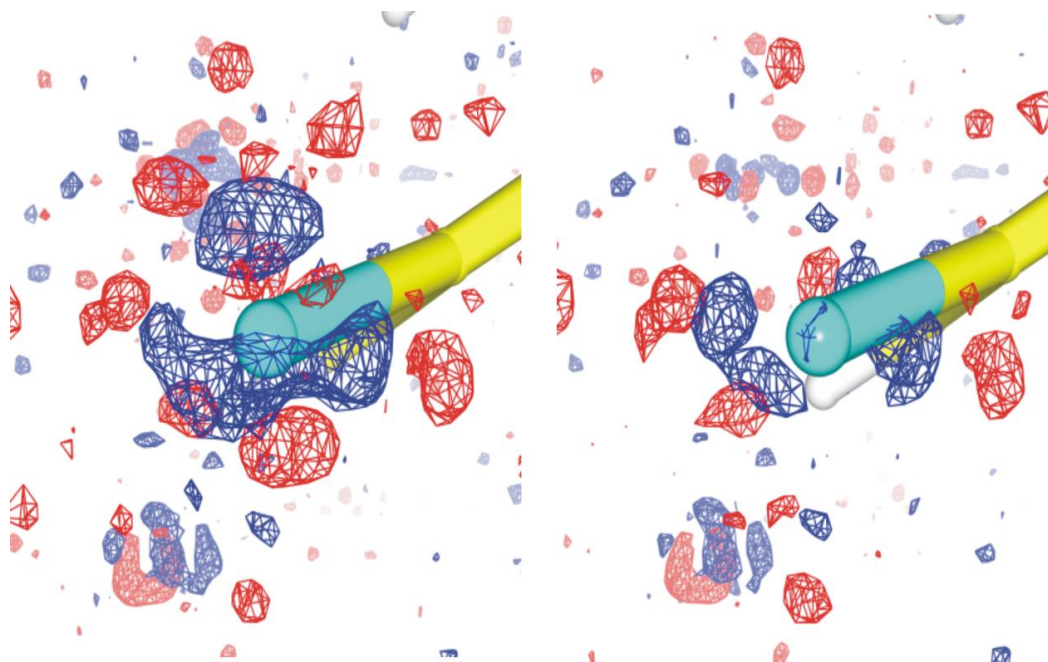


Figure S2. Residual Fourier maps of chlorine atoms surroundings – in harmonic (left) and anharmonic (right) approximation. Isocontour $0.125\text{e}/\text{\AA}^3$, blue positive, red negative.

After reaching convergence in the successive constrained refinement of all parameters, the ADPs for H-atoms were generated by SHADE server [Madsen, 2006] and fixed at these values. Then chemical equivalency and symmetry constraints were changed into restraints with $\sigma = 0.01$ and refined until convergence.

In the final cycles of multipolar refinement the following constraints/restraints were applied:

- (i) H-atoms: ADP's constrained to SHADE values; neutron distances fixed, κ_{hyd} restrained to 1.16 and κ'_{hyd} to 1.20 ($\sigma = 0.05$);
- (ii) Cl1: κ and κ' restrained to 1.000 ($\sigma = 0.003$) due to unreasonably high values and unrealistic deformation density for unrestrained model [following the procedure described by Bui, 2009];
- (iii) P_{lm} 's of the two oxygen atoms O81, O82 restrained to be similar with $\sigma = 0.01$;
- (iv) the ADPs of Br restrained to the values obtained after high/low order refinement of coordinates and thermal motion, with $\sigma = 0.0002$ and charge density parameters constrained to the transferred values;
- (v) P_{val} , P_{lm} , κ and κ' of C91 atom fixed at the transferred values, while for N91 at the carefully redefined values leading to the best residual map.

$\pi \cdots \pi$ stacking														
cp5	C5 _{π}	C5 _{π} ^{vii}	3.2762	1.6381	1.6381	0.055	0.60	-0.17	-0.08	0.85	0.52	13.39	-10.47	2.92
cp6	O82	C71 ⁱⁱ	3.5203	1.6542	1.9186	0.020	0.32	-0.06	-0.04	0.42	0.33	6.32	-3.85	2.47
cp7	C71	C3 _{π} ^{iv}	3.6982	1.9429	1.7811	0.028	0.32	-0.05	-0.03	0.40	0.49	6.53	-4.47	2.06
Weak halogen bonds														
cp8	O82	Cl1 ^{ix}	3.4136	1.6113	1.8042	0.025	0.35	-0.07	-0.05	0.48	0.24	7.06	-4.52	2.54
cp9	O81	Cl1 ^{ix}	3.4555	1.6154	1.8454	0.026	0.40	-0.07	-0.07	0.54	0.04	7.97	-5.04	2.93
cp10	N2 _{π}	Cl1 ^{iv}	3.5690	1.6883	1.8833	0.028	0.37	-0.07	-0.06	0.49	0.11	7.46	-4.95	2.51
cp11	Cl1	Cl1 ^{vi}	3.7301	1.8651	1.8651	0.029	0.36	-0.08	-0.05	0.48	0.33	7.32	-4.94	2.38

Symmetry codes: *i*: x-1/2, -y+3/2, z-1/2; *ii*: -x+1, y+1, -z+2; *iii*: x-1/2, -y+1/2, z+1/2; *iv*: -x+3/2, y-1/2, -z+3/2; *v*: -x+2, -y+1, -z+2; *vi*: -x+2, y+1, -z+1; *vii*: -x+1, -y+1, -z+1; *viii*: x-1/2, -y+1/2, z-1/2; *ix*: x, y, z+1.

Weak $\pi\cdots\pi$ stacking and halogen interactions

The $\pi\cdots\pi$ stacking interactions in **SS1&6** with bond paths and cp's found between $C\cdots C/O/Cl$ atoms ($\rho_{cp} = 0.020 - 0.055 \text{ e}/\text{\AA}^3$ and $\nabla^2\rho = 0.32 - 0.60 \text{ e}/\text{\AA}^5$) are weaker than the antiparallel dipolar contacts, but of similar strength as the halogen bonds described below.

Among the remaining weak contacts, longer than the sum of van der Waals radii, but with well-defined bond paths and critical points found between the interacting atoms, there are two halogen bonds: homoatomic $Cl\cdots Cl$ (cp11, Fig. S3) and heteroatomic, bifurcated $Cl\cdots O$ (cps 8-9, Fig. S4). The first one can be classified as type-I symmetrical interaction [Desiraju & Parthasarathy, 1989] that often occurs around the inversion centre, where the regions of charge concentration are directed towards each other. The strength of this halogen contacts is comparable to the weakest interaction found in hexachlorobenzene [Bui *et al.*, 2009], with the $\rho_{cp} = 0.029 \text{ e}/\text{\AA}^3$ and $\nabla^2\rho = 0.36 \text{ e}/\text{\AA}^5$.

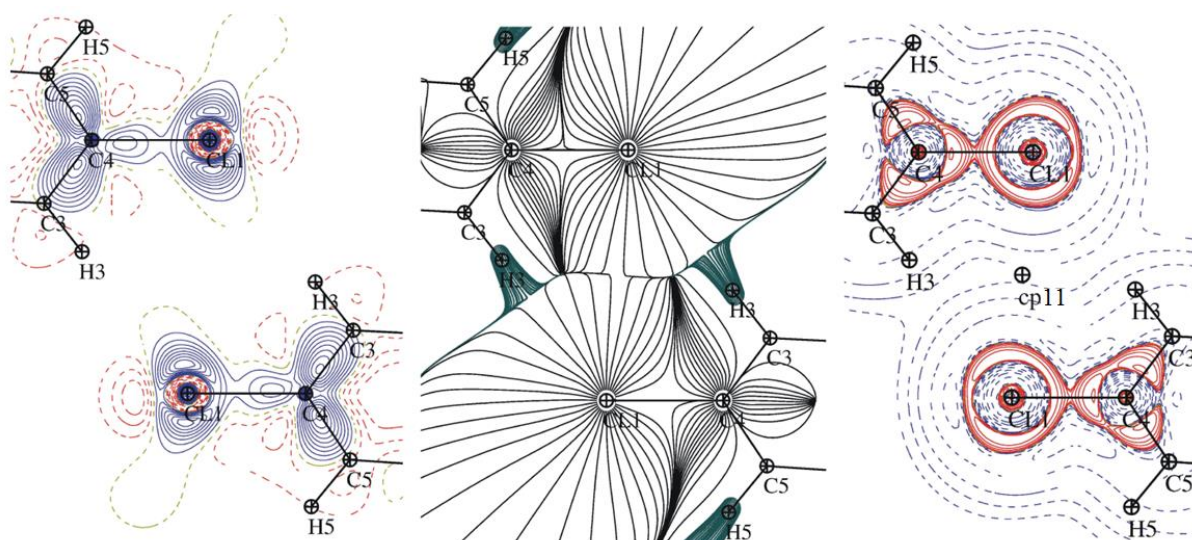


Figure S3. Weak $Cl\cdots Cl$ interaction representation: static deformation density map (left, contours $0.05 \text{ e}/\text{\AA}^3$), total static density gradient map (middle), Laplacian of total electron density (right).

In the bifurcated halogen bond between one chlorine and two oxygen atoms of the same nitro group (cps 8-9), there is one shorter and one longer contact, but the topological descriptor values for both contacts are in the same range as for cp11 and longest heteroatomic halogen bond (cp10):

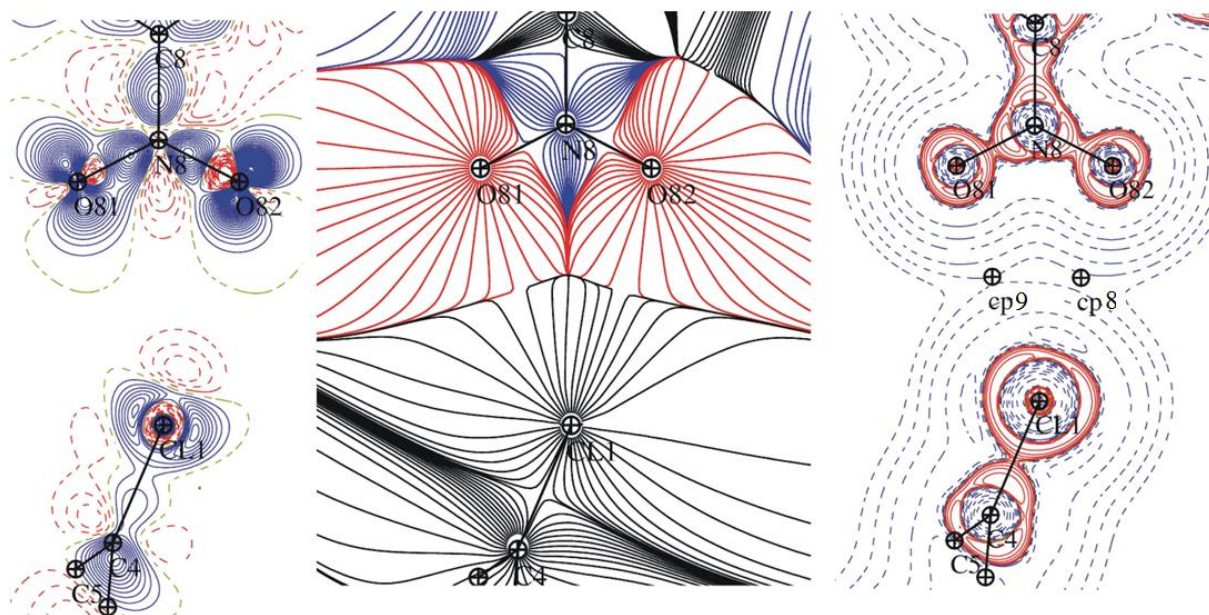


Figure S4. Cl...O interaction representation: static deformation density map (left, contours 0.05 $e/\text{\AA}^3$), total static density gradient map (middle), Laplacian of total electron density (right).

In conclusion for both **SS1&6** and **2**, the antiparallel contact of two cyano groups is the most prominent interaction, there are also three moderate strength hydrogen bonds – slightly stronger in **SS1&6** (**SS1&6**: $\text{C}\equiv\text{N}/\text{O}/\text{Cl}\cdots\text{H}$ with ($\rho_{\text{cp}} = 0.025 - 0.070 \text{ e}/\text{\AA}^3$ and $\nabla^2\rho = 0.58 - 1.06 \text{ e}/\text{\AA}^5$); **2**: $\text{O}/\text{C}\equiv\text{N}/\text{N}_{\text{imidazole}}\cdots\text{H}$ with ($\rho_{\text{cp}} = 0.026 - 0.034 \text{ e}/\text{\AA}^3$ and $\nabla^2\rho = 0.65 - 0.70 \text{ e}/\text{\AA}^5$)). The whole range of weak contacts such as halogen bonds (in **SS1&6**) and stacking (in **SS1&6** and **2**) one can name *tertiary* interactions.

References

- Desiraju, G. R. ; Parthasarathy, R. J. *Am. Chem. Soc.*, 1989, 111, 8725-8726.
- Henn, J., Meindl, K., Schwab, G., Oechsner, A. & Stalke, D. (2010). *Angew. Chem. Int. Ed.* 49, 2422–2426.
- Johnson, C. K. & Levy, H. A. (1974). *Thermal Motion Analysis Using Bragg Diffraction Data. In International Tables for X-ray Crystallography, Vol. IV, pp. 311–336. Birmingham: Kynoch Press.*
- Meindl, K.; Herbst-Irmer R.; Henn, J. *Acta Cryst.* (2010). A66, 362-371.
- Sørensen, H. O., Stewart, R. F., McIntyre, G. J. & Larsen, S. (2003). *Acta Cryst.* A59, 540–550.
- Zhurov, V. V., Zhurova, E. A., Stash, A. I. & Pinkerton, A. A. (2011). *Acta Cryst.* A67, 160–173.